AUT Journal of Electrical Engineering

AUT J. Electr. Eng., 56(1) (Special Issue) (2024) 57-78
DOI: 10.22060/eej.2023.22349.5534

Effective Approach to Use Artificial Intelligence for Detecting Different Faults in Working Electrical Machines

Seyed Hamid Rafiei [1], Mansoor Ojaghi [1]*, Mahdi Sabouri [2]

[1] Department of Electrical Engineering, University of Zanjan, Zanjan, Iran
[2] Department of Electrical and Computer Engineering, Technical and Vocational University (TVU), Tehran, Iran.

ABSTRACT: Artificial intelligence (AI) shows good potential for detecting and discriminating faults in electrical machines, however, they require initial training with sufficient data, which is almost impossible to collect for working electrical machines in the field. This paper proposes an effective approach to solve this problem by getting the required training data from exact simulation results. To evaluate this idea, the finite elements method is used to simulate a three-phase induction motor (IM) in the healthy state as well as the stator inter-turn fault, broken rotor bar fault, and mixed eccentricity fault conditions. Then, for every fault condition, some fault indices are extracted from the stator line current and used to arrange and train a suitable support vector machine (SVM) model to detect and discriminate the fault condition. A similar IM is prepared in the laboratory, where, its stator line currents are sampled and recorded under the healthy and the fault conditions, and the same fault indices are extracted from the stator currents. Some penalties, which are determined by comparing experimental test results and corresponding simulation results in the healthy state, are applied to the experimentally attained values of the indices. The modified indices are then applied to the trained SVM models, where, the attained results confirm the trained SVM models are equally able to detect and discriminate the faults in the real IMs.

Review History:

Received: Apr. 22, 2023
Revised: Jun. 05, 2023
Accepted: Jun. 30, 2023
Available Online: Feb. 01, 2024

Keywords:

Artificial intelligence
Electrical machines
Fault diagnosis
Finite elements method
Training data

1- Introduction

Condition monitoring to detect incipient faults is an undeniable necessity for electrical machines. Many researchers have examined the use of artificial intelligence methods (AIMs) for this purpose. This is due to the potential capability of the AIMs to separate the fault effect in the used fault indices from the effects of the other factors such as the load level change, supply voltage imbalance, distortion, etc. However, the AIMs are often case-sensitive, which means an AIM trained for detecting a fault in an induction motor may not perform exactly for detecting the same fault in another induction motor of the same type and rating. This is due to minor differences in the constructions of the motors, which may present during production and/or assembly processes. In addition, three-phase voltages applied to the stator terminals may include different power quality measures, which affect the used fault indices.

To detect the stator inter-turn short circuit (ISC) fault in induction motors (IMs), some harmonics of the stator current, symmetrical components of the stator current and voltage as well as some graphical indices like the current Concordia pattern (CCP) and the pendulum swing phenomenon (PSP) have been proposed [1-6]. The IM fault classification based on the mentioned indices along with the support vector machine (SVM) model has been widely accepted. Detecting different IM faults by using SVM and kNN methods examined in [7]. The SVM model was trained to detect the stator ISC fault by using experimentally attained voltage imbalance in [8], CCP index in [9], motor current signature analysis (MCSA), and wavelet transform analysis results in [10]. In [11], three different SVM classification models were used to detect the ISC and insulation breakdown faults by considering the voltage imbalance, which demonstrated good accuracy. The ISC fault detection using artificial neural network (ANN) with monitoring experimental data has been studied in [12]. The SVM models were utilized to detect the ISC faults in permanent magnet synchronous motors by using experimental data in [13], in inverter-connected IMs by using simulation results in [14], and also by using experimental data in [15, 16].

Broken rotor bar (BRB) fault and mixed eccentricity (ME) fault indices have been already presented in the machine's instantaneous power [17], stator current [18], rotor force and torque [19, 20], magnetic flux density [21, 22], leakage flux [23] and external magnetic field [24]. Mechanical fault detection in the IMs has been proposed in [25] by using a second-order observer and in [26] through using a multi-sensor fusion scheme. Reference [27] utilized the SVM classification method to identify the rotor bar failure by extracting the harmonic curve level, harmonic crest angle, and harmonic amplitude from the power spectrum density (PSD) of the steady-state stator current. By evaluating several

*Corresponding author's email: mojaghi@znu.ac.ir

harmonic indices on the stator phase current in [28-30] and on the power density spectrum in [27], high percentage of success achieved based on the experimental data. In addition, detection of BRB fault investigated by using experimental current wavelet transform in a SVM model and pattern recognition under different loads [31]. In [32], BRB fault detection with a combined SVM method based on harmonic index and wavelet transform analysis achieved 99% accuracy. A BRB fault detection method based on the SVM with simulation and experimental data presented in [33]. In [34], wavelet transform results and time-amplitude features are utilized in an SVM classification method to investigate eccentricity faults produced due to the inner and outer raceway bearing faults. The eccentricity and bearing faults detection using experimental data and SVM have been examined in [35-39]. Detection of eccentricity resulting from the bearing faults was investigated based on the use of current harmonic amplitudes with experimental data [40] and using a combined SVM-Fuzzy method and three SVM classification methods in [41]. Due to the high advantage of the SVM, this method is also used to investigate detecting IM combined faults. Detection of combined BRB and eccentricity faults has been studied using the multi-label classification method and the machine starting current in [42], using the pattern recognition based on the minimum Bayes error and the stator current in [43], and using ANN and stator current harmonics in [44, 45]. Reference [46] used a decision fusion system (DFS) to classify and reduce the time in investigating the IM states, which includes the healthy motor as well as the motors with the stator short-circuit faults, the rotor unbalancing, the rotor bending, the broken rotor bar, eccentricity, and bearing faults. Then, 6 classification methods including SVM, LDA, kNN, IIS, GMM, and LVQ were used to classify the faults. Reference [47] used the SVM method based on Radial Basic Function (RBF) to detect stator and rotor faults, including asymmetry states, shaft bending, loose of mechanical parts, short circuit, phase imbalance, and broken rotor bars in induction motors. In reference [48], SVM used through Park's vector method to classify the healthy condition from broken rotor bar fault and stator short circuit fault. A comparison between single-class and double-class SVMs performed based on the frequency indices to detect the healthy state form BRB defect, winding ISC and eccentricity defects by considering unbalance supply voltages in [49]. Detection of BRB, static eccentricity (SE), and ME faults separately using frequency indices of the stator current by SVM models and automatic expert system investigated using experimental data in [50]. In addition, using the SVM method to detect ISC, BRB, and eccentricity faults investigated on electric drives of the wind farms in [51].

All the above-mentioned AIMs require initial training with a complete and valid dataset before they can make accurate decisions about the fault occurrence. In most of the above references, the training is based on some experimental data. However, it is not possible to prepare such a dataset for large machines working on production lines. Another noteworthy point in the above references is that in all cases, the training and verification platforms are the same. This means that the proposed AIM goes through the learning process in an experimental or simulation environment, and then, goes through evaluation and testing in the same environment. Therefore, there is no guarantee that it will work in other conditions or for other machines.

This paper proposes an effective approach to using AIMs for diagnosing faults in working electrical machines. According to this approach, the data obtained from simulation are used for training and evaluation of the AIMs. The main requirement for this approach is accurate modeling and simulation of the behavior of healthy and faulty machines in various working conditions. In this paper, the most accurate modeling method available, which is the finite elements method (FEM), is used to simulate the IM behavior under the healthy state, the stator inter-turn short circuit fault, the broken rotor bars fault, and the eccentricity fault conditions. Then, some well-known indexes of the faults are extracted from the stator line currents and used to train and evaluate a suitable SVM model to detect and separate every fault type. Afterward, the same IM is tested in the laboratory under healthy and faulty conditions, and the corresponding fault indexes are extracted from the stator current. The studies indicate that by applying some pre-specified corrections to the indices values extracted from the experimental results, it will be possible to detect and discriminate the real IM faults by using the same SVM models. The required correction to the experimental indices is determined by comparing the healthy state values of the indices in the corresponding experimental and simulation results. As another contribution, the proposed approach brings some generality to the AIM-based fault diagnosis tasks. This is because the IMs of the same type and rating have the same FEM models; therefore, the AIM prepared this way is the same for all the IMs of the same type and rating. However, every individual IM may need a different correction rate for modifying the measured fault indices before applying to the SVM.

2- The SVM Classification Model

As the introduction implies, the SVM classification model has been widely used to detect electrical machine faults. This model is classified as a pattern recognition algorithm that requires supervised learning. The main benefit of the SVM model is that, unlike the ANNs, it does not get trapped in local extremums. This model can provide an acceptable solution for problems with large data and may contain a compromise between the complexity of the classifier and the fault occurrence rate [52]. To be used in the SVM model, the required data set D should contain n members as follows [52]:

$$D = \left\{ (x_i, y_i) \middle| x_i \in R^{\mathrm{P}}, y_i \in \{-1, 1\} \right\}_{i=1}^{n} \quad (1)$$

where x is a p-dimensional real vector containing different variables of a data point and y is the output variable of the SVM model, which classifies the input data point. In the

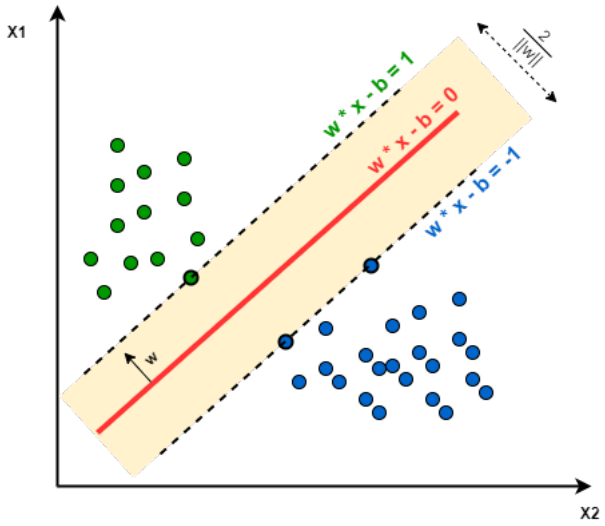

Fig. 1. Illustrating some SVM parameters and concepts [53]

SVM model, the aim is to find the maximum distance of the marginal points or the separating hyperplane that separates the points with y_i=1 from the points with y_i=-1. Each separator hyperplane is a set of x points that satisfy the following condition:

$$w.x - b = 0 \tag{2}$$

where w is a normal vector to the separating plane. The vectors w and b are chosen to bring the maximum distance between two hyperplanes on both sides of the separator hyperplane, which are described by:

$$\begin{aligned} w.x - b &= 1 \\ w.x - b &= -1 \end{aligned} \tag{3}$$

If the data points are linearly separable, it will be possible to include the side hyperplanes on the edge of the points without any common points and then increase their distance to a maximum value. For a double-class dataset in 2-D space (X1, X2), Fig.1 shows the data points, the separating plane (designated by $w.x_i$-b=0), the side plains (designated by $w.x_i$-b=1 and $w.x_i$-b=-1), the vector normal w and the geometrical distance between the two side planes (2/||w||) that is also called the margin. The data point vectors located on the side planes are called support vectors. The margin is maximized by minimizing ||w||. To prevent data points from entering the margin, the following conditions must be satisfied:

$$\begin{aligned} w.x_i - b &\geq 1 \ , \text{if} \ \ y_i = 1 \\ w.x_i - b &\leq -1, \text{if} \ \ y_i = -1 \end{aligned} \tag{4}$$

that are also expressed as follows:

$$y_i (w.x_i - b) \geq 1, \ \forall 1 \leq i \leq n \tag{5}$$

Considering the constraint (5), an optimization problem obtains as follows to determine w and b vectors:

$$\begin{aligned} &\min_{(w,b)} \|w\| \\ &s.t. \ \ y_i (w.x_i - b) \geq 1 \ \ ; \ \ \forall 1 \leq i \leq n \end{aligned} \tag{6}$$

Alternatively, ||w|| can be replaced by $||w||^2/2$ to attain a nonlinear optimization problem:

$$\begin{aligned} &\min_{(w,b)} \frac{1}{2}\|w\|^2 \\ &s.t. \ \ y_i (w.x_i - b) \geq 1 \ \ ; \ \ \forall 1 \leq i \leq n \end{aligned} \tag{7}$$

Using non-negative Lagrange coefficients (α_i), the above equation can be written as follows:

Table 1. Technical data of the IM

Parameter	Value
Rated Power	1.1 [kW]
Rated Voltage	380 [V]
Rated Frequency	50 [Hz]
Pole Pairs	2
Connection	Y
Stator Slots Number	36
Rotor Slots Number	28
Healthy Air Gap Length	0.3 [mm]
Air Gap Mean Radius	40 [mm]
Stack Length	60 [mm]
Stator Winding Turn Per Coil	63 [Turn]
Stator Resistance Per Phase	7.8 [Ω/Phase]
Rotor Bar Resistance	9.72 [μΩ]
End Ring Resistance	8 [μΩ]
Leakage inductance of Stator	18.8 [mH/Phase]
Leakage inductance of Rotor Bar	0.571 [μH]
Leakage inductance of End Ring	0.051 [μH]
Inertia Moment	0.002385 [Kg.m^2]
Winding Scheme of Phase "A"	
A-1-12'-2-11'-3-10'-19-30'-20-29'-21-28'-X	

$$\min_{(w,b)} \max_{(\alpha)} \left\{ \frac{1}{2}\|w\|^2 - \sum_{i=1}^{n} \alpha_i (y_i (w.x_i - b) - 1) \right\} \quad (8)$$

To find saddle points, the problem is solved using standard nonlinear programming, where the answer can be expressed as a linear combination of learning data vectors:

$$w = \sum_{i=1}^{n} \alpha_i y_i x_i \quad (9)$$

Only a few α_i will be greater than zero. The corresponding x_i will be exactly the support vector that will satisfy the condition. Therefore, the support vectors must fulfill the following conditions:

$$y_i (w.x_i - b) = 1 \quad (10)$$

Then. the vector b is defined as follows:

$$b = \frac{1}{N_{sv}} \sum_{i=1}^{N_{sv}} (w.x_i - y_i) \quad (11)$$

where N_{sv} is the average of all the support vectors, which makes the algorithm more robust. More details about the SVM method are available in [52].

3- Dataset Preparation:

Two extensive datasets are prepared: one dataset from simulation results and the other dataset from experimental test results. Each dataset contains required data of the healthy and defective IMs with ISC, BRB, and ME faults by considering balanced and unbalanced three-phase supply voltages. The first dataset is prepared through simulation using FEM. A part of this dataset is used for SVM training and the other part is used for its testing and evaluation. After obtaining the desired result from the training and evaluation by the first dataset, another evaluation is performed using the second dataset. By obtaining the desired result from the second evaluation, the ability to detect faults in the real IMs using the trained SVMs is confirmed.

3- 1- Preparation of Simulation Dataset

Ansys Maxwell-2D software is used to prepare the simulation dataset. The behavior of the healthy and faulty IMs under the ISC, BRB, and ME faults with different severities is simulated by considering balanced and unbalanced supply voltages. Then, some well-known indices of the mentioned faults are evaluated and analyzed to verify the simulation results. The simulations are performed for a 1.1 kW, 380

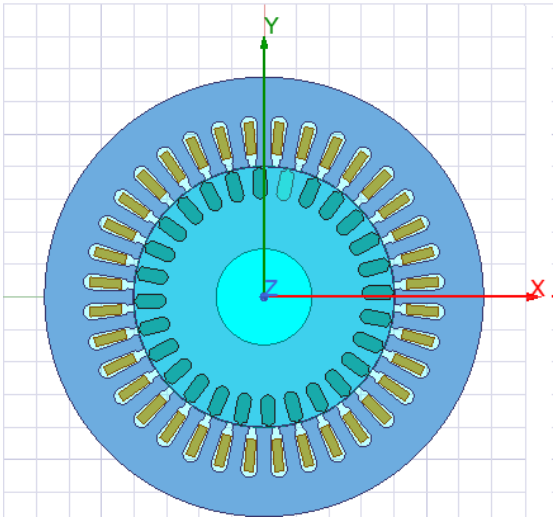

Fig. 2. Induction motor simulated in Ansys Maxwell software with a broken rotor bar

Fig. 3. Photographs of the laboratory setup

V, 50 Hz, 4-pole IM with a star connection. Table 1 shows the technical data of the IM. The RMxprt feature of Ansys Electronic Desktop 2020 is used to design a healthy IM according to the specifications given in Table 1 and also according to the structural and dimensional features of the proposed IM. To model the stator ISC fault, the number of shorted turns is reduced from the number of coil turns in the corresponding slots of the stator. To apply the ME fault, the Maxwell Eccentricity feature embedded in the Maxwell ACT Extensions Wizards is used with desired degrees. The BRB fault is applied by simply removing the broken rotor bar from the 2-D FEM model as shown in Fig. 2.

3- 2- Preparation of Experimental Dataset

To prepare the experimental dataset, a real IM with the same specifications as presented in Table 1 is used, on which, it is possible to apply the ISC, BRB, and ME faults temporarily. Fig. 3 shows the aforementioned experimental set-up, where the mentioned induction motor is coupled to a synchronous generator to apply the load to the motor. To prevent the IM from being affected by the possible eccentricity of the synchronous generator, a special disc coupling with a clamp connection type DMPA-C is used [54]. Fig. 4 shows a photograph of this coupling device. The stator terminals of the synchronous generator are connected to a variable resistive load bank. By changing the resistance of the load bank, the load of the induction motor is adjusted. To sample and record the stator line voltages and currents, DAQ card type PCI-1716, along with current sensors type LTS6-NP and voltage sensors type LV25-P are used along with the LabView-V2012 software.

To apply the BRB fault, a rotor containing the required number of broken bars replaces the healthy rotor. A rotor bar breaks by drilling on it. Fig. 5 shows photographs of the rotors, where the healthy rotor is located at the top, the rotor with 1 broken bar is at the middle and has two holes on a rotor

Fig. 4. Photograph of the proposed coupling devise

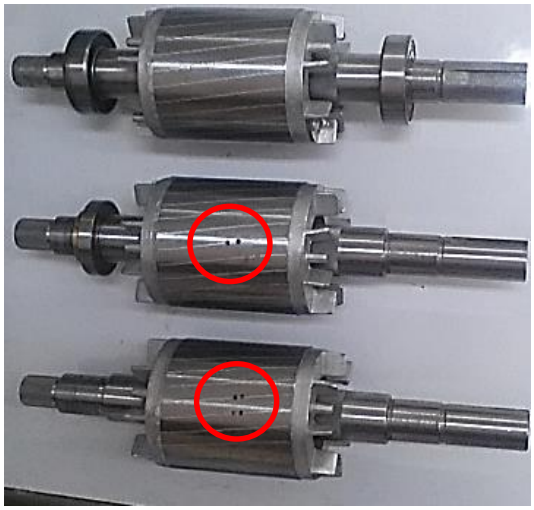

Fig. 5. Top to bottom: photograph of the healthy rotor, photograph of the rotor with one broken bar, and photograph of the rotor with two broken bars.

bar and the rotor with 2 broken bars is at the bottom and has four holes on two bars (two holes on every bar).

To create ME fault, the original bearings of code 6205 are temporarily substituted with bearings of code 6906. Compared to the original bearing, the new bearing has a larger inner diameter and a smaller outer diameter. The inner and outer diameters mismatch of the new bearing is compensated by making and installing suitable rings inside and outside it. Now, if the used rings have eccentricity, which means that the inner and outer circles of the ring do have not the same center, it will cause mixed eccentricity in the motor. The positions of the thinnest and thickest points of the rings are tagged on them at manufacturing time. This allows aligning the bearings on both ends of the rotor when installation to prevent creating inclined eccentricity. Fig. 6 shows photographs of the original bearing code 6205, substituted bearing code 6906, and fabricated outer and inner rings.

To create the stator winding ISC fault, a number of taps are extracted from various turns of a stator coil. By shorting every two extracted taps, temporary ISC fault is produced with different severities from 2 turns up to 32 turns.

4- Preparing SVM Models to Detect Faults

In this section, three separate SVM models are prepared using the simulation dataset to diagnose and discriminate stator ISC fault, BRB fault, and mixed eccentricity fault, respectively. Then, the models are evaluated with the rest of the simulation dataset. In the following, the evaluation is performed with the experimental dataset. Finally, each SVM model is evaluated with experimental data related to the other two faults. In all cases for the SVM model, the box constraint for the Soft Margin is equal to 10 and the kernel function is considered to be a Radial Basic Function with a sigma (scaling factor) value of 0.7.

Fig. 6. Left to right: photograph of the fabricated inner ring, photograph of the fabricated outer ring, photograph of the new bearing code 6906 and photograph of the original bearing code 6205

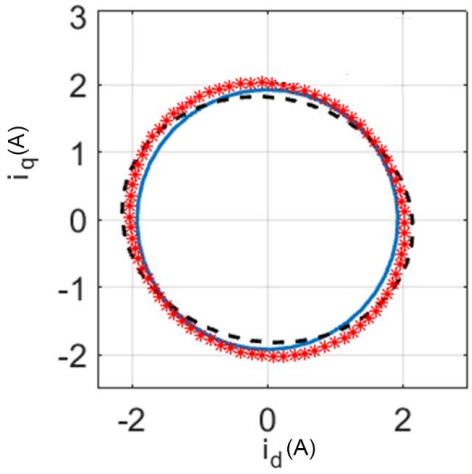

Fig. 7. The current Concordia pattern for healthy IM with balanced supply voltages (—), healthy IM with unbalanced supply voltages (***), and defective IM with 20-turns shorted in a stator phase winding (---)

4- 1- Stator ISC Fault Detection using SVM

Various indices and methods have been examined in the literature to detect the stator ISC fault in three-phase IMs. In this article, the current Concordia pattern is employed for this purpose [3, 4, 12]. In a healthy state with balanced three-phase supply voltages, the mentioned pattern is a circle, but the occurrence of the ISC fault or the supply voltage imbalance causes its shape to change to an ellipse. Fig. 7 shows the current Concordia pattern for the intended IM in healthy conditions with balanced/unbalanced supply voltages and in ISC fault conditions with balanced supply voltages, which are calculated and drawn using the fundamental harmonic of the stator currents resulting from the simulation. As can be seen, the current Concordia pattern is a visual index to detect the ISC fault; however, a quantitative index is needed to be utilized in the SVM model. In this study, the major diameter (MaD) to minor diameter (MiD) ratio of the ellipse is considered a quantitative measure. In order to make it possible to separate the effects of the supply voltage imbalance and the stator ISC fault, there is a need for another criterion. In this study, the amplitude of the negative sequence voltage (NSV) component of the stator is selected for this purpose. Therefore, the proposed SVM model will have two inputs: the MaD/MiD ratio of the Concordia pattern ellipse and the amplitude of the NSV component in the stator supply voltage.

Using the simulation dataset, 30 samples of the current Concordia pattern are extracted and utilized for the SVM training. Table 2 introduces the samples. A rather weak ISC fault condition, which includes 2 shorted turns, is applied for training because this makes detection of the severer faults more reliable. Fig. 8-a shows the SVM model training result. Then, 70 other samples are used for the initial evaluation of the trained SVM model. The conditions of the samples exploited for evaluation are presented in Table 3. Fig. 8-b

Table 2. The samples employed to train the SVM model in different conditions

SCIM Condition	Negative Sequence Component of the Supply Voltage (V)					Number of samples
	0	2	4	8	12	
Healthy	√					7
Healthy		√				2
Healthy			√			2
Healthy				√		2
Healthy					√	2
2-turns shorted	√					7
2-turns shorted		√				2
2-turns shorted			√			2
2-turns shorted				√		2
2-turns shorted					√	2
Total Training Samples						30

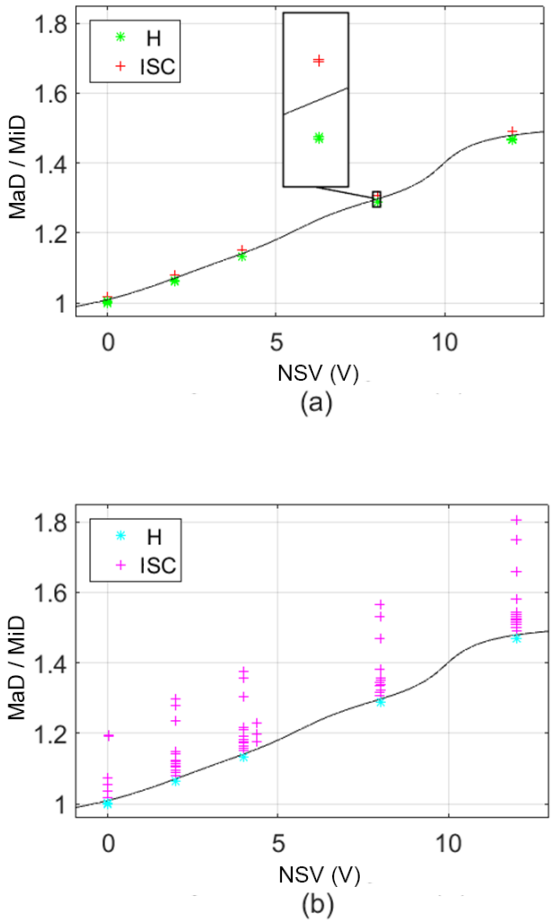

Fig. 8. The training of the SVM model for ISC fault detection based on simulation data: a) training result, b) initial evaluation result)

Table 3. Samples used for initial evaluation of the trained SVM model with simulation results

SCIM Condition	Negative Sequence Component of the Supply Voltage (V)					Number of samples
	0	2	4	8	12	
Healthy	√					6
Healthy		√				2
Healthy			√			2
Healthy				√		2
Healthy					√	2
2-turns shorted	√					3
2-turns shorted		√				1
2-turns shorted			√			1
2-turns shorted				√		1
2-turns shorted					√	1
4-turns shorted	√					3
4-turns shorted		√				1
4-turns shorted			√			1
4-turns shorted				√		1
4-turns shorted					√	1
6-turns shorted	√					3
6-turns shorted		√				3
6-turns shorted			√			3
6-turns shorted				√		3
6-turns shorted					√	3
8-turns shorted	√					3
8-turns shorted		√				3
8-turns shorted			√			3
8-turns shorted				√		3
8-turns shorted					√	3
20-turns shorted	√					3
20-turns shorted		√				3
20-turns shorted			√			3
20-turns shorted				√		3
Total Evaluation Samples						70

shows the evaluation result, where the accuracy of fault diagnosis reaches 100%.

The trained SVM model is then evaluated using experimental results. To obtain accurate results before this evaluation, it is necessary to inspect the correspondence of the behavior of the healthy motor in the simulation and experimental results. For this purpose, 10 samples of the current Concordia pattern acquired from the experimental results in the healthy state are applied to the trained SVM model. Fig. 9-a shows the result. As can be seen, the gravity center of the samples for the healthy experimental results is placed away from the SVM separator compared to the gravity center of the healthy samples from the simulation results (Fig.8-a). This is due to some simplifying assumptions in the simulation, such as using two-dimensional FEM, ignoring the rotor bars skewing effect, and inherent asymmetry of the real IM. Sampling errors in the experimental test results should also be added to the above reasons. The investigation shows to create a relative correspondence for the desired application of the trained SVM model; it is required to correct the ratio of the diameters of the Concordia pattern ellipse obtained from the experimental results with a fixed correction factor. After applying this correction factor, 20 experimental samples consisting of 10 samples from the healthy IM and 10 samples from the defective IM with different fault severities are studied. Table 4 shows the conditions of the experimental samples used in this evaluation. As can be seen, the mains electricity system, which supplies the IM in the laboratory, includes different negative sequence voltage components between 2 to 4 volts. Fig. 9-b shows the result of the evaluation of the trained SVM model for healthy and faulty experimental data, which indicates that the diagnostic accuracy is equal to 100%.

Table 4. Experimental samples used to evaluate the SVM model

SCIM Condition	Negative Voltage (V)	Number of samples	SCIM Condition	Negative Voltage (V)	Number of samples
Healthy	2.77	1	2-turns shorted	2.40	1
Healthy	2.91	1	4-turns shorted	2.60	1
Healthy	3.11	1	6-turns shorted	2.64	1
Healthy	3.15	1	8-turns shorted	2.66	1
Healthy	3.18	1	10-turns shorted	2.80	1
Healthy	3.20	1	12-turns shorted	2.86	1
Healthy	3.32	1	14-turns shorted	3.11	1
Healthy	3.40	1	16-turns shorted	3.20	1
Healthy	3.73	1	18-turns shorted	3.30	1
Healthy	4.00	1	20-turns shorted	3.54	1
Total Evaluation Samples		10	Total Evaluation Samples		10

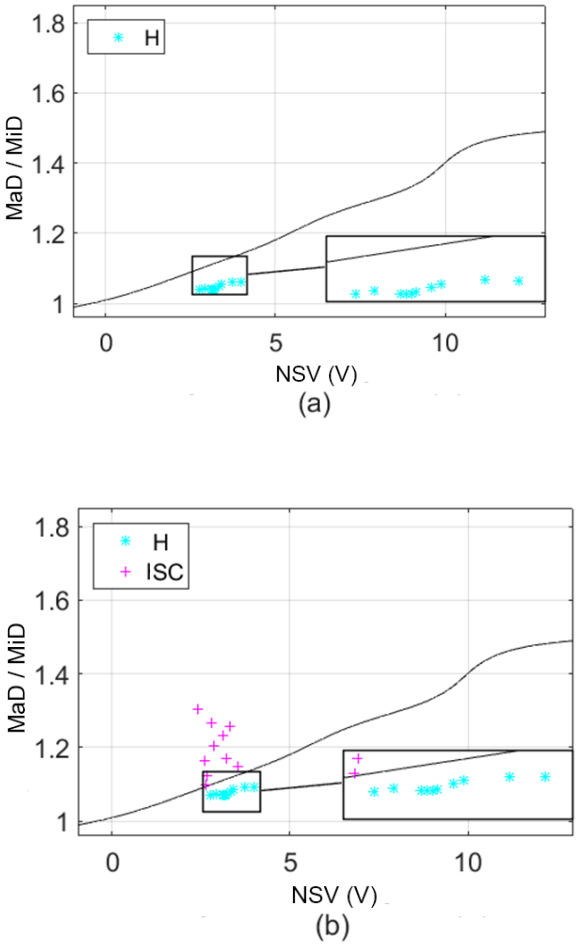

Fig. 9. Final evaluation of the SVM trained for ISC fault detection by using experimental data: a) healthy samples before correction, b) healthy and defective samples after correction

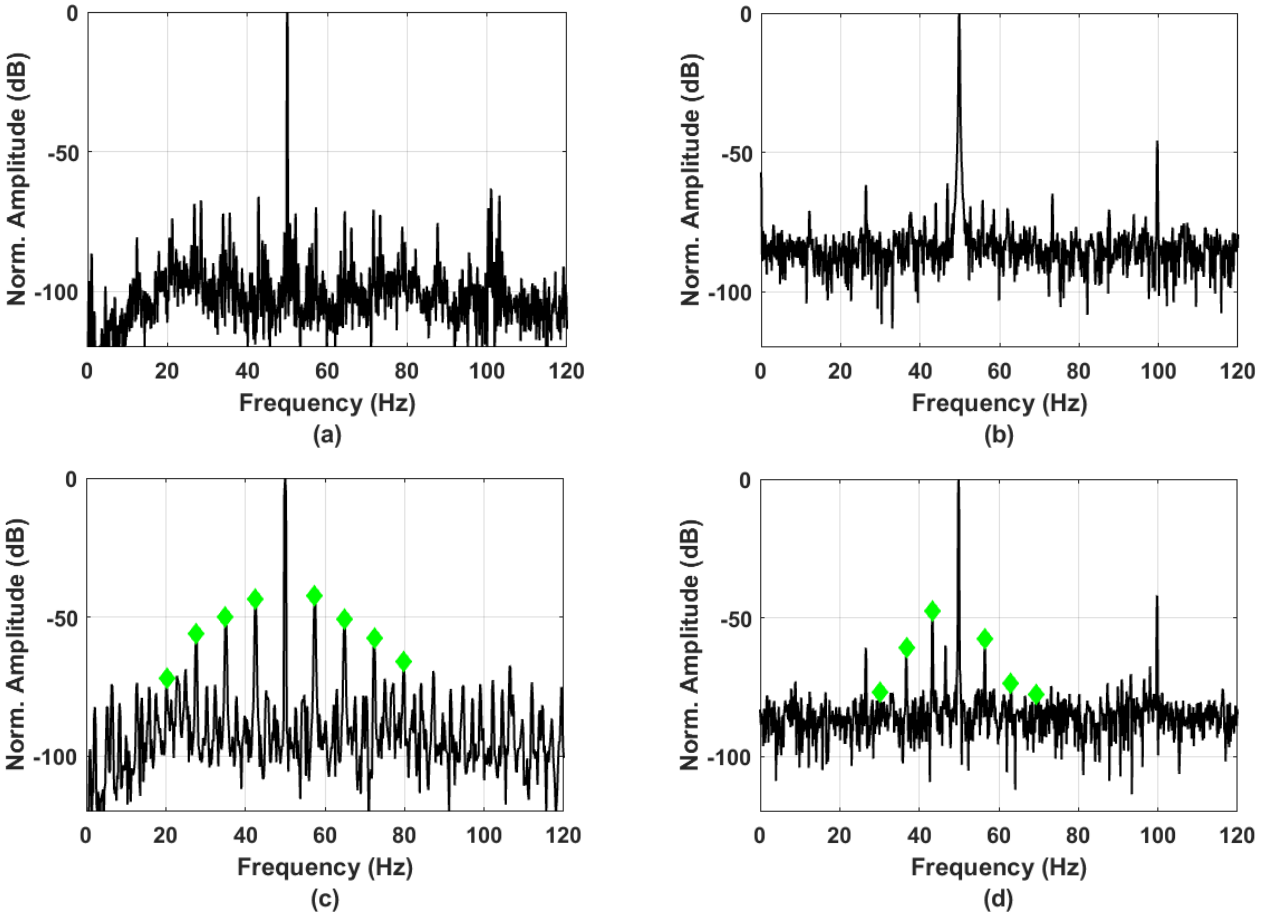

Fig. 10. Normalized frequency spectra of the stator current attained through simulation (left column) and experimental tests (right column) under Healthy (first row) and 1-BRB (second row) fault condition that indicates the BRB-related sidebands with sign (♦)

4- 2- BRB Fault Detection using SVM

The BRB fault adds some harmonics to the stator current spectrum whose exact frequencies are computed by [5, 6]:

$$f_{bb} = |1 \pm 2ks| f_s \tag{12}$$

where s is the slip, k=1, 2, … and f_s is the fundamental frequency. These harmonics can be used to discriminate between the healthy state and the BRB fault condition. For instance, Fig. 10 shows the stator current normalized spectra in the healthy and 1-BRB fault conditions. Although some of the BRB-related harmonics exist in a healthy state, the BRB fault causes a significant increase in their amplitudes. For k=1, two frequencies $f_{bb}^{-} = |1-2s| f_s$ and $f_{bb}^{+} = |1+2s| f_s$ obtain from (12), which are the lower and higher sideband frequencies of the BRB fault. In this article, the normalized amplitudes (in dB) of these two frequency components are appointed as the input of the SVM model. A dataset consisting of 54 simulation samples is arranged to train and evaluate the SVM model for BRB fault detection. This dataset includes 24 samples of the healthy IM and 30 samples of the defective IM with one or two BRBs. Among the dataset, 24 samples are employed to train the SVM model, which includes 12 samples of the healthy state and 12 samples of the defective state. The result of the SVM training is shown in Fig. 11-a. The rest of the samples are utilized for the initial evaluation of the SVM model, which includes 12 and 18 samples for the healthy and the defective states, respectively. Fig. 11-b shows the result of the evaluation, where it is evident that the accuracy rate of the evaluation is as high as 100%. In the following, the trained SVM model is evaluated using experimental results. Before this evaluation, it is necessary to examine the required matching between the proposed frequency components of the healthy IM in the corresponding

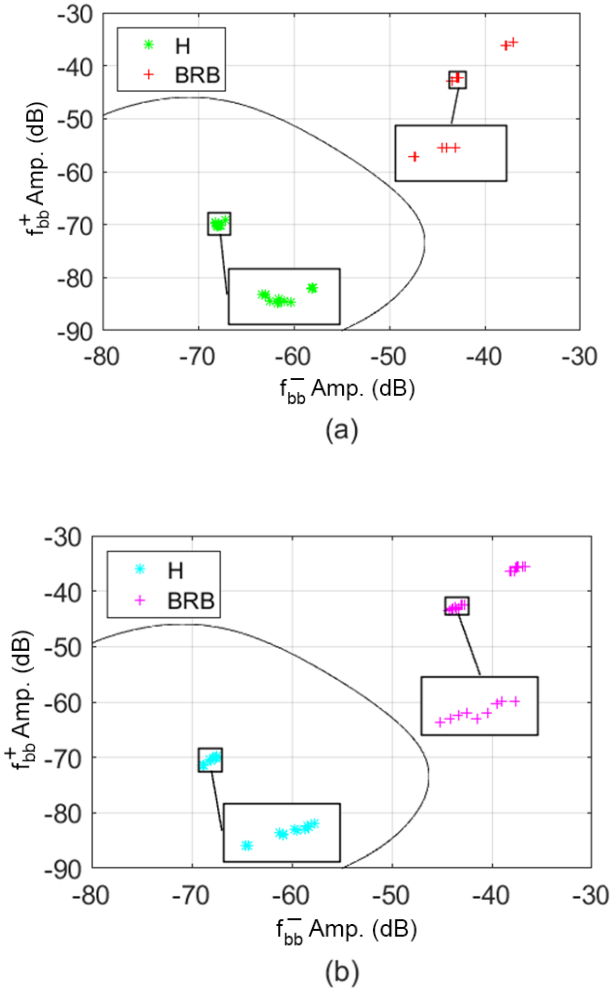

Fig. 11. The training of the SVM model for BRB fault detection based on simulation data: a) training result, b) initial evaluation result

simulation and experimental results. For this purpose, 10 experimental samples of the healthy state are applied to the trained SVM model, as shown in Fig. 12-a. It is clear that the gravity center of the healthy experimental samples has a slight displacement compared to the gravity center of the healthy simulation samples, such that, the experimental samples are slightly away from the SVM separator curve. This difference is due to some simplifications and ignoring some effects in modeling and simulation, as mentioned in the previous subsection. Investigation shows that to make good compliance, a fixed correction factor should be applied to the normalized amplitudes of the frequency indices collected from the experimental results. By applying this modification, 30 experimental samples including 10 healthy state samples and 20 defective state samples with one and two BRBs are studied. Fig. 12-b shows the result of the evaluation of the trained SVM model for the healthy and the defective experimental data, which indicates an accuracy rate of 100%.

4- 3- ME Fault Detection by SVM

The ME fault adds harmonics to the stator current whose frequencies are calculated by [1]:

$$f_{me} = |f_s \pm k f_r| \tag{13}$$

where k=1, 2, …, f_s is the fundamental frequency, and f_r is the rotor speed frequency. Substituting k=1 gives two sidebands around the fundamental harmonic with equal distances, which are named the higher sideband (HSB) and the lower sideband (LSB). These two harmonics are the main indices for detecting the ME fault in the IMs. Fig. 13 shows the stator current normalized spectra obtained through simulation and

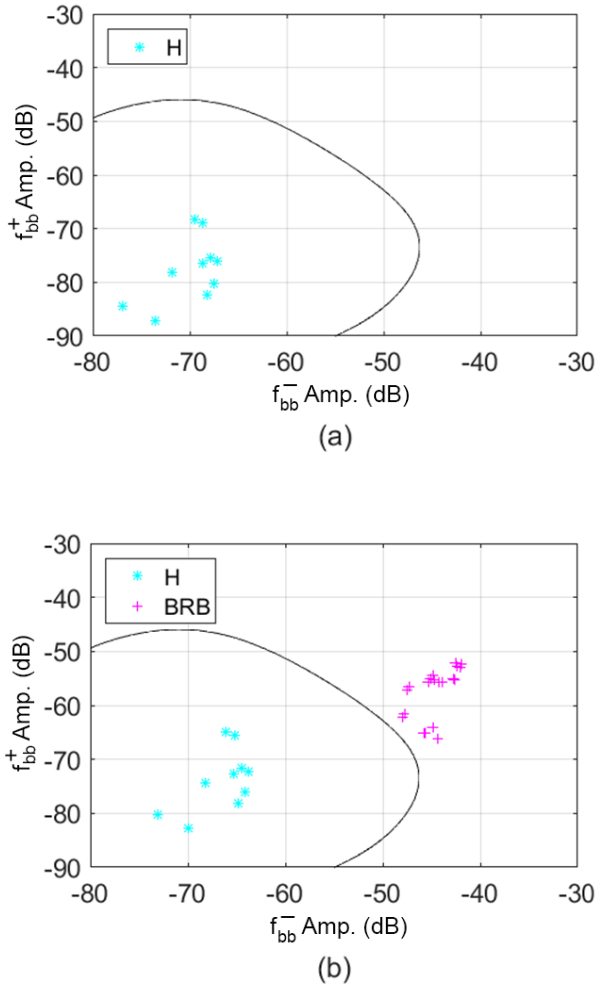

Fig. 12. Final evaluation of the SVM trained for BRB fault detection using experimental data: a) healthy samples before correction, b) healthy and defective samples after correction

experiments under a healthy state and a ME fault condition with 30% static and 20% dynamic components. The presence or amplification of the two mentioned sidebands due to the ME fault are evident in both the simulation and experimental results.

The normalized amplitudes of the two sidebands are selected as the input to the SVM model. A dataset consisting of 87 simulation samples is selected to train and evaluate the SVM model for the ME fault diagnosis. This dataset consists of 27 healthy samples and 60 ME samples with static and dynamic components from 5% to 20%. A set of 24 samples are applied to train this SVM model, which includes 12 samples of the healthy motor and 12 samples of the defective motor. Fig. 14-a shows the training result. The remaining 63 samples are utilized for the initial evaluation of this SVM model. Fig. 14-b shows the evaluation result. As can be seen, the accuracy of the initial evaluation of this model is 100%.

Subsequently, the trained SVM model is evaluated by employing experimental results. Before this evaluation, like the previous two subsections, it is necessary to match the gravity center of the healthy experimental results to that of the simulation results. It is performed by modifying the normalized amplitudes of the two sidebands in the experimental results. For this purpose, 20 experimental samples of the healthy motor are employed. The attained modification is applied identically in all healthy and defective samples. By applying this modification, 50 experimental samples were studied, which consisted of 20 healthy samples and 30 defective samples with different eccentricity degrees including 30% static & 20% dynamic, 15% static & 25% dynamic, 40% dynamic, 20% dynamic, and 40% static. Fig. 15 shows the result of the evaluation of the trained SVM model for experimental data, which indicates an accuracy rate of 98.6%. It should be noted that we often encounter ME

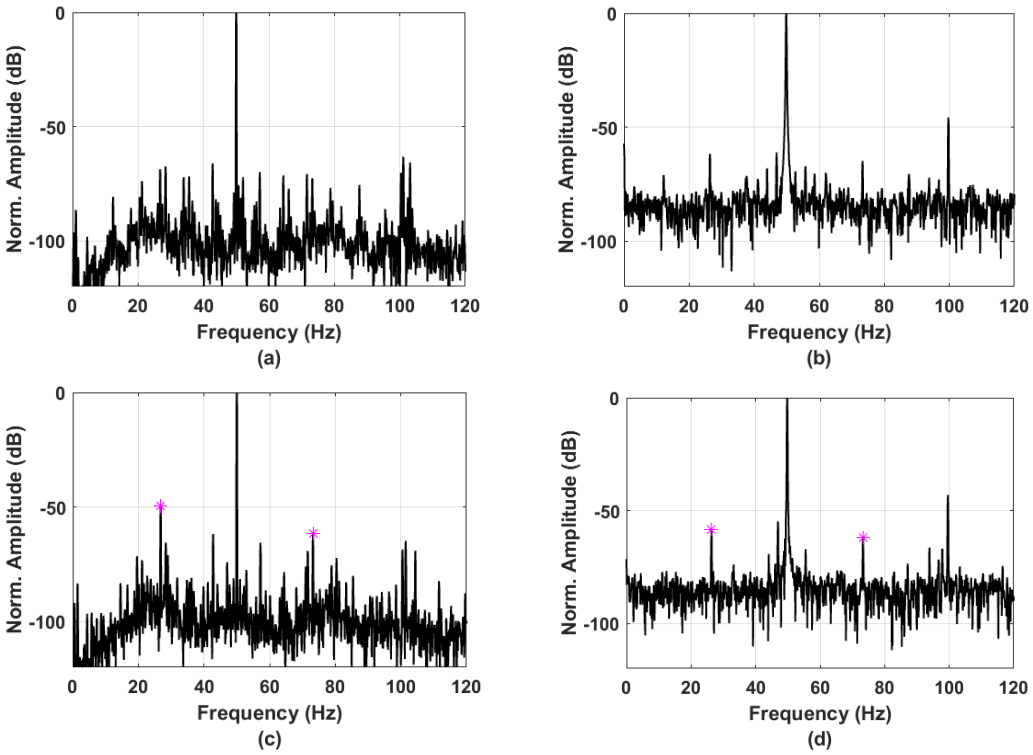

Fig. 13.Normalized frequency spectra of the stator current attained through simulation (left column) and experimental tests (right column) under Healthy (first row) and ME fault (second row) condition that indicates the ME-related sidebands with sign (*)

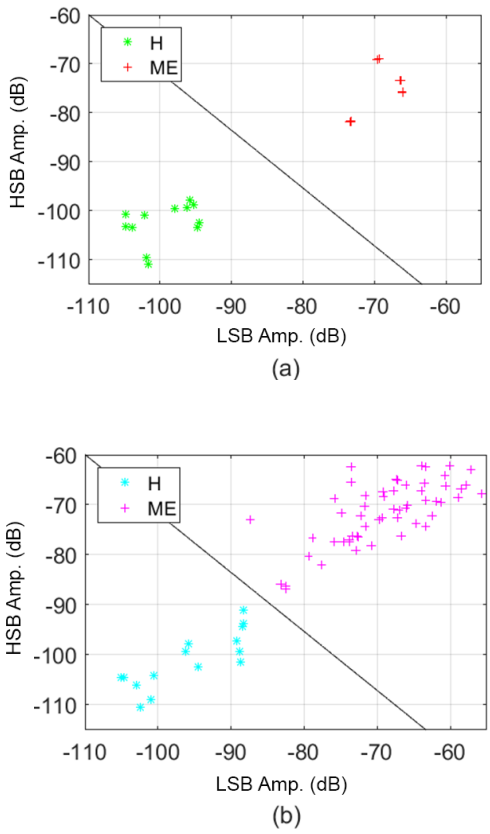

Fig. 14. The training of the SVM model for ME fault detection based on simulation data: a) training result, b) initial evaluation result

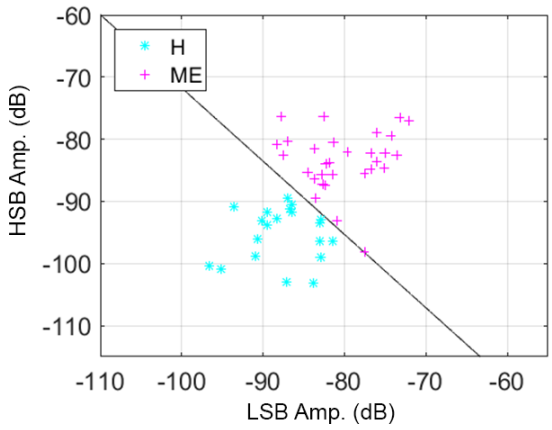

Fig. 15. Final evaluation of the SVM trained for the ME fault detection by using the healthy and the defective experimental data

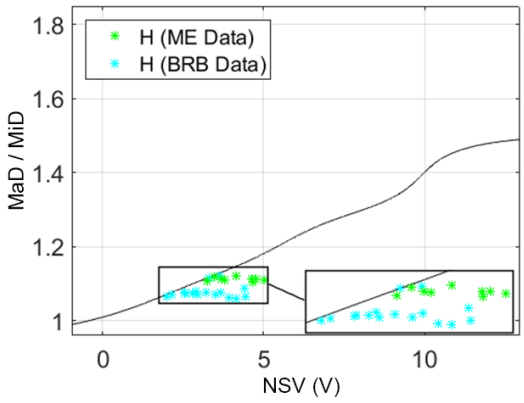

Fig. 16. Examining the SVM model trained for detecting ISC faults against the BRB and ME faults.

fault because of the inherent eccentricity of the real IM, even if it is required to create pure static or dynamic eccentricity.

4- 4- Examining Stability of the SVM Models against Other Fault Conditions

In this section, every trained SVM model is examined against fault conditions that it has not been trained to detect them. This examination is accomplished using experimental data to verify possible misdiagnosis of the proposed faults. In every case, the related modifications as mentioned in the previous subsections are applied to the experimental results before applying them to the SVM models. Fig.16 shows the examination result of the SVM model trained to detect the ISC fault against the experimental BRB and ME fault samples. As demonstrated, this SVM model does not classify the ME or BRB fault samples as defective ones, therefore, the ME and BRB defects are not classified as the ISC fault.

Fig. 17 shows the examination result of the SVM model trained to detect the BRB fault against the ISC fault and the ME fault experimental samples. As can be seen, the SVM model classifies all the samples as the healthy state; therefore, the ISC or ME fault cannot be classified as the BRB fault. Fig. 18 presents the examination result of the SVM model trained to detect the ME fault against the ISC fault and

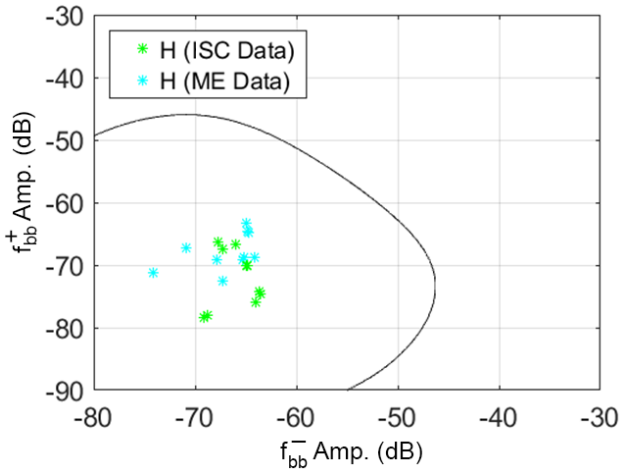

Fig. 17. Examining the SVM model trained for detecting BRB fault against the ISC and ME faults.

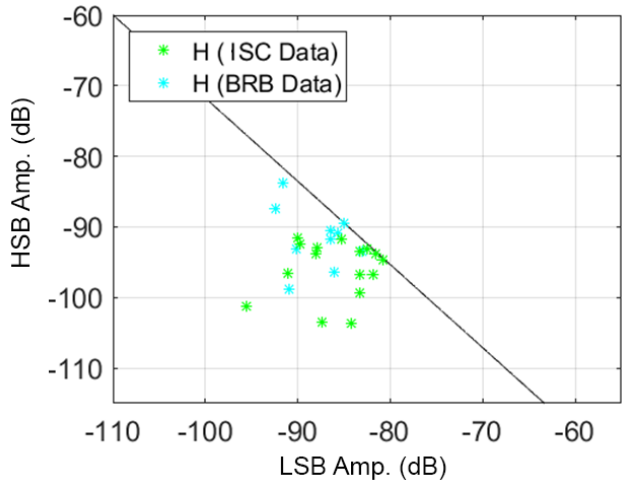

Fig. 18. Examining the SVM model trained for detecting ME fault against the ISC and BRB faults.

BRB fault experimental samples. As it is obvious, the SVM model trained for ME fault detection evaluates the ISC and BRB faults as healthy conditions; therefore, an ISC or BRB fault is not classified as the ME defect. Overall functions and procedures to arrange the proposed fault diagnosis technique are illustrated in Fig. 19.

5- Conclusion

A new approach was proposed and examined for diagnosing different faults in induction motors using an artificial intelligence method that is the support vector machine model, in which, FEM simulation results were utilized to train and pre-evaluate the model. The trained SVM model for every fault condition was able to detect the same fault in the same real induction motor if the fault indices values extracted from the stator currents of the real motor had been modified using appropriate coefficients. The coefficients were determined to bring the experimental values of the indices in the healthy state to their corresponding values attained through simulation. Classification accuracies up to 100% are reached when diagnosing the faults in real induction motors. The attained SVM models were stable against the other fault conditions for which they were not trained.

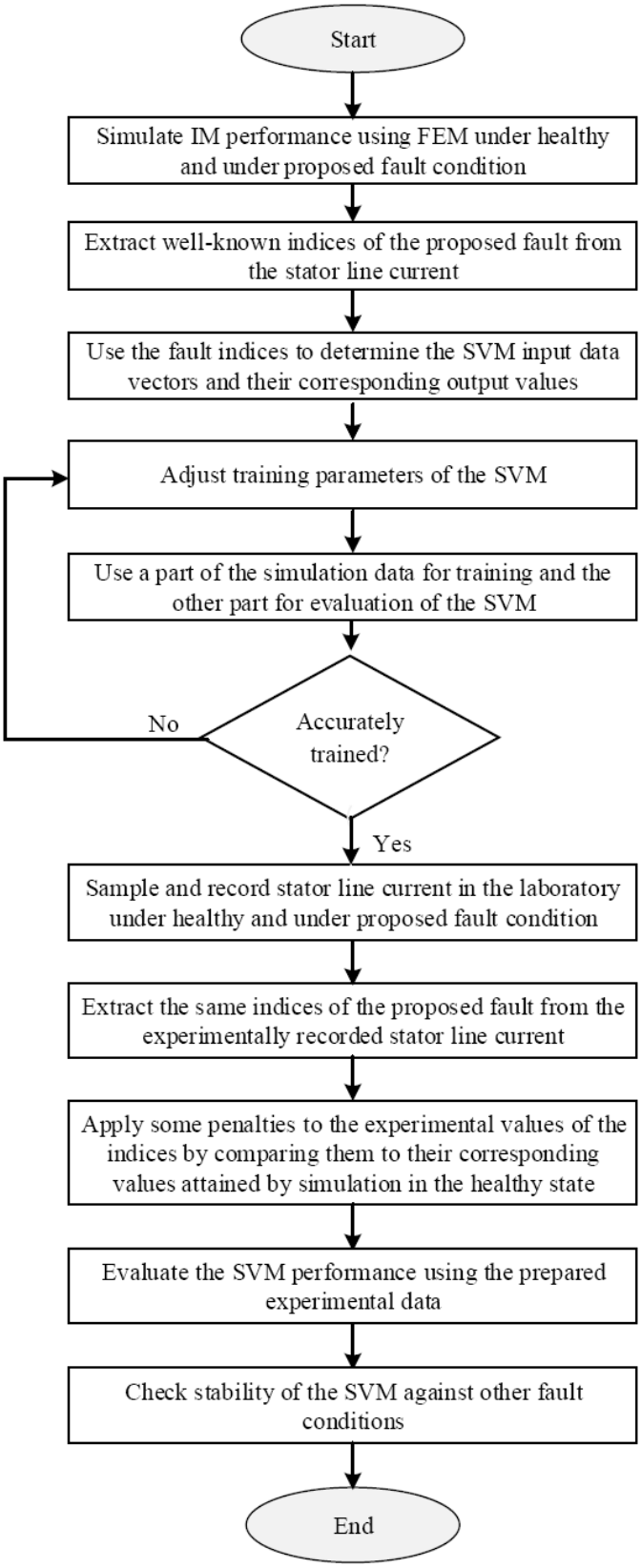

Fig. 19. Overall procedure to arrange the proposed fault diagnosis technique

Nomenclature

SVM	Support vector machine
AIM	Artificial intelligence method
IM	Induction motor
ISC	Inter-turn short circuit
CCP	Current Concordia pattern
PSP	Pendulum swing phenomenon
kNN	K-nearest neighbors
MCSA	Motor current signature analysis
NSV	Negative sequence voltage
BRB	Broken rotor bar
ME	Mixed eccentricity
PSD	Power spectrum density
DFS	Decision fusion system
LDA	Linear discriminant analysis
GMM	Gaussian mixture model
LVQ	Learning vector quantization
IIS	Improved iterative scaling
RBF	Radial basic function
SE	Static eccentricity
FEM	Finite elements method
sigma	Sigma parameter of RBF
D	Dataset
x_i	SVM input vector
y_i	SVM output vector
w	Normal vector
b	Bias parameter
α_i	Non-negative Lagrange coefficients
N_{sv}	Average of all the support vectors
DAQ	Data Acquisition
H	Healthy situation
MiD	Minor diameter
MaD	Major diameter
s	Motor slip
f_s	Fundamental frequency
f_{bb}	BRB index frequency
f_{bb}^-	BRB lower sideband frequency
f_{bb}^+	BRB higher sideband frequency
f_{me}	ME index frequency
f_r	Rotor speed frequency
LSB	ME lower sideband frequency
HSB	ME higher sideband frequency

References

[1] E. Solodkiy, D. Dadenkov, "Detection of Stator Inter-turn Short Circuit in Three- Phase Induction Motor Using Current Coordinate Transformation", 2019 26th International Workshop on Electric Drives: Improvement in Efficiency of Electric Drives (IWED), IEEE, DOI: 10.1109/IWED.2019.8664353, Jan 30-Feb 02, 2019.

[2] H.B. Bostan Abad, M. Ojaghi, A. Taheri, "Efficient Index for Detecting the Stator Winding Interturn Fault in Six-Phase Squirrel Cage Induction Motors", DOI: 10.1016/j.measurement.2021.109912 , 0263-2241/© 2021 Elsevier Ltd., 18 July 2021.

[3] M. Ojaghi, M. Sabouri, J. Faiz, "Performance Analysis of Squirrel-Cage Induction Motors Under Broken Rotor Bar and Stator Inter-Turn Fault Conditions Using Analytical Modeling", IEEE Transactions on Magnetics, DOI:10.1109/TMAG.2018.2842240, vol. 54, no. 11, Nov. 2018.

[4] M. Y. Kaikaa, M. Hadjami, A. Khezzar, "Effects of the simultaneous presence of static eccentricity and broken rotor bars on the stator current of induction machine," IEEE Trans. Industrial Electronics, DOI: 10.1109/TIE.2013.2270216, vol. 61, no. 5, pp. 2452-2463, May 2014.

[5] A. Toliyat, S. Nandi, S. Choi, and H. Meshgin-Kelk, "Electric machines modeling, condition monitoring, and fault diagnosis", U.S.: Taylor & Francis Group, eBook Number-13: 978-1-4200-0628-5, Jan. 2012.

[6] M.B.K. Bouzid; G. Champenois, "Neural Network Based Method for the Automatic Detection of the Stator Faults of the Induction Motor", 2013 Inter. Conference on Electrical Engineering and Software Applications, IEEE, DOI: 10.1109/ICEESA.2013.6578393, 15 Aug. 2013.

[7] S. Sridhar, K. Uma Rao, R. Umesh; K. S. Harish, "Condition Monitoring of Induction Motor using Statistical Processing", 2016 IEEE Region 10 Conference (TENCON), DOI: 10.1109/TENCON.2016.7848597, 22-25 Nov. 2016.

[8] J. Seshadrinath, B. S. Fellow, B. K. Panigrahi, "Incipient Turn Fault Detection and Condition Monitoring of Induction Machine using Analytical Wavelet Transform", 2012 IEEE Industry Applications Society Annual Meeting, DOI: 10.1109/IAS.2012.6374026, 07-11 Oct. 2012.

[9] S. Das, C. Koley, P. Purkait, and S. Chakravorti, "Wavelet aided SVM Classifier for Stator InterTurn Fault Monitoring in Induction Motors", IEEE PES General Meeting, DOI: 10.1109/PES.2010.5589595, 25-29 July 2010.

[10] Dr. Jagadanand G, Fedora Lia Dias, "ARM Based Induction Motor Fault Detection Using Wavelet and Support Vector Machine", 2015 IEEE International Conference on Signal Processing, Informatics, Communication, Energy Systems (SPICES), DOI: 10.1109/SPICES.2015.7091503, 19-21 Feb. 2015.

[11] S. Das, P. Purkait, C. Koley, and S. Chakravorti "Performance of a Load-immune Classifier for Robust Identification of Minor Faults in Induction Motor Stator Winding", IEEE Trans. on Dielectrics and Electrical Insul., DOI 10.1109/TDEI.2013.003549, vol. 21, no. 1, Feb. 2014.

[12] M. Mohamed, E. Mohamed, A. Mohamed, and M.M. Hassan, "Detection of Inter Turn Short Circuit Faults in Induction Motor using Artificial Neural Network", 2020 26th Conference of Open Innovations Ass. (FRUCT), DOI: 10.23919/FRUCT48808.2020.9087535, June 21,2020.

[13] K.J. Shih, M.F. Hsieh, B. J. Chen, and S.F. Huang, "Machine Learning for Inter-turn Short-circuit Fault Diagnosis in Permanent Magnet Synchronous Motors", IEEE Transactions on Magnetics, DOI: 10.1109/TMAG.2022.3169173, 21 April 2022.

[14] A. Vinayak, R. Uddin, and Dr. Jagadanaand, "Inter phase fault detection in inverter fed Induction motor using wavelet transform",2017 3rd International Conference on Condition Assessment Tech. in Electrical Sys. (CATCON), IEEE, DOI: 10.1109/CATCON.2017.8280193, 16-18 Nov. 2017.

[15] C. Delpha, H. Chen, and D. Diallo, "SVM based diagnosis of inverter fed induction machine drive a new challenge", IECON 2012 - 38th Annual Conference on IEEE Industrial Electronics Society, DOI: 10.1109/IECON.2012.6389264, 20 Dec. 2012.

[16] F. Husari, and J. Seshadrinath, "Incipient Inter Turn Fault Detection and Severity Evaluation in Electric Drive System Using Hybrid HCNN-SVM Based Model", IEEE Transactions on Industrial Informatics, DOI: 10.1109/TII.2021.3067321, vol.18, Issue. 3, March 2022.

[17] Z. Liu, X. Yin, and others, "Online Rotor Mixed Fault Diagnosis Way Based on Spectrum Analysis of Instantaneous Power in Squirrel Cage Induction Motors", IEEE Trans. on Energy Conversion, DOI: 10.1109/TEC.2004.832052, vol. 19, Issue. 3, pp. 485 - 490, 24 Aug. 2004.

[18] I. Ishkova, O. Vítek, "Diagnosis of eccentricity and broken rotor bar related faults of induction motor by means of motor current signature analysis", 2015 16th International Scientific Conference on Electric Power Engineering (EPE), DOI: 10.1109/EPE.2015.7161130, 978-1-4673-6788-2/15/$31.00 ©2015 IEEE, 20-22 May 2015.

[19] V. Fireteanu, A. I. Constantin; A. Zorig, and A. Chouder, "Impact of the Stator Short-circuit, Rotor Broken Bar and Eccentricity Faults on Rotor Force for Loaded and No-load Induction Motors Operation," 2018 Inter. Conference on Applied and Theoretical Electricity (ICATE), DOI: 10.1109/ICATE.2018.8551471, 978-1-5386-3806-4/18/$31.00 ©2018 IEEE, 29 Nov. 2018.

[20] V. Fireteanu, A.I. Constantin, and M. Popa, "Influence of Single or Multiple Faults Short-circuit, Broken Rotor Bar and Eccentricity on the Torque and Rotor Force in Induction Motors", 2018 XIII International Conference on Electrical Machines (ICEM), DOI: 10.1109/ICELMACH.2018.8507008, 978-1-5386-2477-7/18/$31.00 ©2018 IEEE, 25 Oct. 2018.

[21] A. Seghiour, T. Seghier, and B. Zegnini, "Diagnostic of the Simultaneous of Dynamic Eccentricity and Broken Rotor Bars Using the Magnetic Field Spectrum of the air-gap for an Induction Machine", 2015 3rd International Conference on Control, Engineering & Information Technology (CEIT), DOI: 10.1109/CEIT.2015.7233158, 03 Sep. 2015.

[22] R. R. Schoen, and T.G. Habetler, "Effects of time-varying loads on rotor fault detection in induction machines," Conference Record of the 1993 IEEE Industry Applications Conference Twenty-Eighth IAS Annual Meeting, in Con& Rec. 28th Annu. IAS Meeting, pp. 324-330, DOI: 10.1109/IAS.1993.298943, 02-08 Oct. 1993.

[23] J. A. Daviu, A. Q. López, Others, "Evaluation of the detectability of rotor faults and eccentricities in induction motors via transient analysis of the stray flux", 2017 IEEE Energy Conversion Congress and Exposition (ECCE), DOI: 10.1109/ECCE.2017.8096633, 978-1-5090-2998-3/17/$31.00 ©2017 IEEE, 07 Nov. 2017.

[24] A. Ceban, R. Pusca, and R. Romary, "Eccentricity and Broken Rotor Bars Faults Effects on the External Axial Field,", The XIX Inter. Conf. on Electrical Machines - ICEM 2010, DOI: 10.1109/ICELMACH.2010.5608009, 978-1-4244-4175-4/10/$25.00 ©2010 IEEE, 25 Oct. 2010.

[25] A. Pilloni, A. Pisano, E. Usai, and R. Panadero, "Detection of rotor broken bar and eccentricity faults in induction motors via second order sliding mode observer", 2012 IEEE 51st IEEE Conference on Decision and Control (CDC), DOI: 10.1109/CDC.2012.6426640, 978-1-4673-2064-1/12/$31.00 ©2012 IEEE, 10-13 Dec. 2012.

[26] G. Luo, T. G. Habetler, and J. Hurwitz, "A Multi-sensor Fusion Scheme for Broken Rotor Bar and Airgap Eccentricity Detection of Induction Machines", 2019 IEEE Energy Conversion Congress and Exposition (ECCE), DOI: 10.1109/ECCE.2019.8912275, 978-1-7281-0395-2/19/$31.00 ©2019 IEEE, 28 Nov. 2019.

[27] M. G. Armaki, and R. Roshanfekr, "A New Approach for Fault Detection of Broken Rotor Bars in Induction Motor Based on Support Vector Machine," 2010 18th Iranian Conference on Electrical Engineering, IEEE, DOI: 10.1109/IRANIANCEE.2010.5506976, 11-13 May 2010.

[28] H. Keskes, A. Braham, and Z. Lachiri, "On the use of Stationary Wavelet Packet Transform and Multiclass Wavelet SVM for Broken Rotor Bar detection", IECON 2012 - 38th Annual Conference on IEEE Industrial Electronics Society, DOI: 10.1109/IECON.2012.6389266, 978-1-4673-2421-2/12/$31.00 ©2012 IEEE, 20 Dec. 2012.

[29] D. Matić, F. Kulić, and others, "Design of Support Vector Machine Classifier for Broken Bar Detection," 2012 IEEE International Conference on Control Applications, DOI: 10.1109/CCA.2012.6402374, 978-1-4673-4505-7/12/$31.00 ©2012 IEEE, 03-05 Oct. 2012.

[30] D. Matić, F. Kulić, "SVM Broken Bar Detection Based on Analysis of Phase Current", 2012 15th International Power Electronics and Motion Control Conference (EPE/PEMC), DOI: 10.1109/EPEPEMC.2012.6397456, 978-1-4673-1972-0/12/$31.00©2012 IEEE, 04-06 Sep. 2012.

[31] S. E. Zgarni, and A. Braham, "Intelligent Induction Motor Diagnosis System: A new challenge", 2016 2nd International Conference on Advanced Technologies for Signal and Image Processing (ATSIP), DOI: 10.1109/ATSIP.2016.7523125, 978-1-4673-8526-8/16/$31.00 ©2016 IEEE, 21-23 March 2016.

[32] H. Keskes, and A. Braham, "Recursive Undecimated Wavelet Packet Transform and DAG SVM for Induction Motor Diagnosis", IEEE Transactions on industrial informatics, DOI: 10.1109/TII.2015.2462315. vol. 11, no. 5, PP: 1059 – 1066, Oct. 2015.

[33] C. M. Pezzani, J. M. Fontana, and Others, "SVM-Based System for Broken Rotor Bar Detection in Induction Motors", 2018 IEEE ANDESCON, DOI: 10.1109/ANDESCON.2018.8564627, 06 Dec. 2018.

[34] H. O. Vishwakarma, K. Sajan, and Others, "Intelligent Bearing Fault Monitoring System Using Support Vector Machine and Wavelet Packet Decomposition for Induction Motors", 2015 International Conference on Power and Advanced Control Engineering (ICPACE), DOI: 10.1109/ICPACE.2015.7274969, 12-14 Aug. 2015.

[35] J. Zarei, M. M. Arefi, and H. Hassani, "Bearing Fault Detection Based on Interval Type-2 Fuzzy Logic Systems for Support Vector Machines", 2015 6th International Conference on Modeling, Simulation, and Applied Optimization (ICMSAO), DOI: 10.1109/

ICMSAO.2015.7152214, 978-1-4673-6601-4/15$31.00 c 2015 IEEE, 27-29 May 2015.

[36] A. Choudhary, D. Goyal, and S. S. Letha, "Infrared Thermography based Fault Diagnosis of Induction Motor Bearings using Machine Learning", IEEE Sensors Journal, DOI: 10.1109/JSEN.2020.3015868, 1530-437X (c) 2020 IEEE, vol. 21, Issue. 2, 15 Jan. 2021.

[37] F. B. Abid, S. Zgarni, and A. Braham, "Bearing Fault Detection of Induction Motor Using SWPT and DAG Support Vector Machines", IECON 2016 - 42nd Annual Conference of the IEEE Industrial Electronics Society, DOI: 10.1109/IECON.2016.7793237, 978-1-5090-3474-1/16/$31.00 ©2016 IEEE, 23-26 Oct. 2016.

[38] S. Gunasekaran, S. Esakimuthu, and Others, "Condition Monitoring and Diagnosis of Outer Raceway Bearing Fault using Support Vector Machine", 2018 Condition Monitoring and Diagnosis (CMD), DOI: 10.1109/CMD.2018.8535744, 23-26 Sep. 2018.

[39] F. B. Abid, S. Zgarni, and A. Braham, "Distinct Bearing Faults Detection in Induction Motor by a Hybrid Optimized SWPT and aiNet-DAG SVM", IEEE Transactions on energy conversion, DOI: 10.1109/TEC.2018.2839083, vol. 33, no. 4, Dec. 2018.

[40] S. E. Pandarakone, K. Akahori, and Others, "Development of a Methodology for Bearing Fault Scrutiny and Diagnosis using SVM", 2017 IEEE International Conference on Industrial Technology (ICIT), DOI: 10.1109/ICIT.2017.7913097, 978-1-5090-5320-9/17/$31.00©2017 IEEE, 22-25 March 2017.

[41] H. Hassani, J. Zarei, and Others, "zSlices–Based General Type–2 Fuzzy Fusion of Support Vector Machines with Application to Bearing Fault Detection", IEEE transactions on industrial electronics, DOI: 10.1109/TIE.2017.2688963, vol. 64, Issue. 9, Sep. 2017.

[42] G. Georgoulas, V. Climente, and others, "Detection of Broken Bars and Mixed Eccentricity Faults Using the Start-up Transient", 2016 IEEE 14th International Conference on Industrial Informatics (INDIN), DOI: 10.1109/INDIN.2016.7819198, 978-1-5090-2870-2/16/$31.00 ©2016 IEEE, 19-21 July 2016.

[43] M. Haji, and H.A. Toliyat, "Pattern Recognition – "A Technique for Induction Machines Rotor Fault Detection Eccentricity and Broken Bar Fault"", Conference Record of the 2001 IEEE Industry Applications Conference. 36th IAS Annual Meeting (Cat. no.01CH37248), DOI: 10.1109/IAS.2001.955745, 0-7803-7116-X/01/$10.00 (C) 2001 IEEE, 30 Sep.- 04 Oct. 2001.

[44] H. Singh, M. Seera, and M. Z. Abdullah, "Detection and Diagnosis of Broken Rotor Bars and Eccentricity Faults in Induction Motors Using the Fuzzy Min-Max Neural Network", The 2013 International Joint Conf. on Neural Networks (IJCNN), DOI: 10.1109/IJCNN.2013.6707003, 04-09 Aug. 2013.

[45] S. Hamdani, O. Touhami, and Others, "Neural Network technique for induction motor rotor faults classification –Dynamic eccentricity and broken bar faults", 8th IEEE Symposium on Diagnostics for Electrical Machines, Power Electronics & Drives, DOI: 10.1109/DEMPED.2011.6063689, 978-1-4244-9303-6/11/$26.00 ©2011 IEEE, 05-08 Sep. 2011.

[46] G. Niu, T. Han, and Others, "Multi-agent decision fusion for motor fault diagnosis", Mechanical Systems and Signal Processing, doi.org/10.1016/j.ymssp.2006.03.003, vol. 21, Issue. 3, pp. 1285-1299, April 2007.

[47] V. A. D. Silva, and R. Pederiva, "Fault detection in induction motors based on artificial intelligence", Federal University of S˜ ao Jo˜ ao del Rei, Corpus ID: 16694089, 2013.

[48] I. Aydin, M. Karakose, and E. Akin, "Artificial Immune Based Support Vector Machine Algorithm for Fault Diagnosis of Induction Motors", 2007 International Aegean Conf. on Electrical Machines and Power Elec., DOI: 10.1109/ACEMP.2007.4510505, 10-12 Sep. 2007.

[49] E. Smart, D. Brown , and L. Axel-Berg, "Comparing One and Two Class Classification Methods for Multiple Fault Detection on an Induction Motor" , 2013 IEEE Symposium on Industrial Electronics & Applications, DOI: 10.1109/ISIEA.2013.6738982, 22-25 Sep. 2013.

[50] J. B. Valencia, M. P. Sanchez, and Others, "Study of Performance of Several Techniques of Fault Diagnosis for Induction Motors in Steady-State with SVM Learning Algorithms", 2014 2nd International Conference on Artificial Intelligence, Modelling and Simulation, DOI 10.1109/AIMS.2014.47, 978-1-4799-7600-3/14 $31.00 © 2014 IEEE, 18-20 Nov. 2014.

[51] S. T. Kandukuri, S. L. Senanyaka, and Others, "A Two-Stage Fault Detection and Classification Scheme for Electrical Pitch Drives in Offshore Wind Farms using Support Vector Machine", IEEE Transactions on Industry Applications, DOI 10.1109/TIA.2019.2924866, 0093-9994 (c) 2019 IEEE, vol. 55, Issue. 5, Sept.-Oct. 2019.

[52] D. G. pascual, "Artificial Intelligence Tools: Decision Support Systems in Condition Monitoring and Diagnosis", Taylor & Francis Group, an informa businessno claim to original u.s. government, 20150225, Ebook – pdf: 978-1-4665-8406-8, April 22, 2015.

[53] Online available: https://www.analyticsvidhya.com/blog/2021/05/multiclass-classification-using-svm/

[54] Oskoyi Ballbering Co. "Oskoyi Ballbering catalogue," https://www.1obc.com/ P.R.C., pp. 11-16, Mar. 2019.

HOW TO CITE THIS ARTICLE

S. H. Rafiei, M. Ojaghi, M. Sabouri, Effective Approach to Use Artificial Intelligence for Detecting Different Faults in Working Electrical Machines. AUT J Electr Eng, 56(1) (Special Issue) (2024) 57-78.

DOI: 10.22060/eej.2023.22349.5534